Contents

A Brief History of Radio Astronomy

Radio Astronomy began in the December of 1932 when Karl Jansky of Bell Labs made the first successful detection of astronomical radio emission coming from the center of our galaxy, The Milky Way. Grote Reber, intrigued by Jansky's discovery made a 30-foot antenna with his own many and succesfully mapped radio emissions from the galaxy at a resolution higher than that of Jansky's. He identified the locations in the sky of several secondary peaks in signal strength in addition to the strong emission from the center of the Milky Way: one in the constellation Cassiopeia (which we now refer to as Cas A and which is known to be a super nova remnant) and another in Cygnus (Cyg A, a radio galaxy). His results were published in 1940 and1944 and were the first radio wavelength observations published in an astronomical journal.

For military reasons, during World War II, there were significant technological developments in radar.After the war J.S. Hey, in collaboration with S. J. Parson, J. W. Phillips, and G. S. Stewart, continued with radar and radio studies and made a number of discoveries. In 1945,Hey and colleagues discovered that meteors leave trails of ionization that reflect radio waves. In 1946,they mapped the radio sky in greater detail than that made by Reber and found that the radio emission observed toward Cygnus varied with time. They recognized Cyg A as a discrete source, distinct from the extended radio emission associated with the Milky Way. In 1948,they determined that the solar radio bursts were associated with sunspots and solar flares.

The realization of a major avenue for study of large pieces of the universe using radio observations was initiated in 1944 when the famous theoretical Dutch astrophysicist Jan Oort suggested to Hendrik van de Hulst that he calculate the wavelength of the emission line of hydrogen due to the spin flip of the electron. The calculations by van de Hulst predicted that this transition should emit radiation at 21 cm wavelength. The first detection of the 21-cm line was made in 1951 by Harold Ewen and Edward Purcell at Harvard. The 21-cm line is still used extensively to map the distribution of hydrogen atoms throughout space.

In 1946, as the first step in the long development of a high-resolution radio astronomy observing technique, Sir Martin Ryle and D. D. Vonberg made the first astronomical observation using a pair of radio antennas as an interferometer. Later interferometric observations by a number of investigators yielded precise measurements of the positions of the bright radio sources.During the 1960s, radio astronomy yielded discoveries of quasars, pulsars, and the cosmic microwave background, with the last two discoveries yielding Nobel Prizes.

Recap of Radiation Physics

2.1 Plank's Function and Rayleigh-Jeans Approximation

In the module on Radiation Physics, we had learned how the radiation emitted from a blackbody can be modelled as a cloud of photons of the same temperature as the body itself.The energy distribution function of photons, (Number of photons as a function of their energy) is directly related to spectral distribution, i.e. Intensity v/s Frequency.

$$B_\nu = \frac{2h\nu^3}{c^2}\frac{1}{e^{\frac{h\nu}{kT}} - 1}$$

Where,
h is the Plank's Constant,
k is the Boltzmann Constant,
c is the Speed of Light,
ν is the frequency of observation, and
T is the temperature of radiating body in Kelvins

At most radio wavelengths, the Planck function can be approximated by a much simpler expression, which makes for much easier math when using it. This approximation will also lead to an extremely important definition of *Brightness Temperature*. At most radio wavelengths,the frequency, ν, is so small that $\frac{h\nu}{kT} << 1$ for any reasonable temperature . The exponential in the denominator of the Planck function then can be approximated by a Taylor series expansion, yielding

$$\frac{1}{e^{\frac{h\nu}{kT}} - 1} \approx \frac{kt}{h\nu}$$

and so,

$$B_\nu \approx \frac{2h\nu^3}{c^2}\frac{kT}{h\nu} = \frac{2k\nu^2 T}{c^2}$$

This expression is very useful, provided you are in the realm where $\frac{h\nu}{kT} << 1$. This expression is known as the Rayleigh–Jeans approximation, as we have seen before and is often referred to as the Rayleigh–Jeans law.At centimeter wavelengths, most of the time we can use the Rayleigh–Jeans approximation, avoiding the far more complex Planck function. Only at the highest radio frequencies

and with observations of cold objects does the approximation start to differ from the full expression. This is one major convenience of working at radio wavelengths. Therefore, Rayleigh-Jeans Approximation is one of the most important equations in Radio Astronomy.

2.1.1 Units of Flux Density

For astronomical sources at radio frequencies, the amount of energy we receive per unit time, per unit area, and per unit bandwidth is incredibly small, so both the SI and the cgs systems yield awkwardly small numbers for typical flux densities. To avoid carrying around excessively negative powers of 10 in our calculations, radio astronomers have defined a unit of flux density, named after the father of radio astronomy, Karl Jansky. In units of the SI system, a *jansky* is defined as

$$1 janksy = 10^{-26} W m^{-2} Hz^{-1}$$

2.2 Brightness Temperature

Brightness Temperature is the property of the radiation and is equal to the temperature of the blackbody that would have produced that radiation. brightness temperature is a measure of intensity, and is equal to the temperature that the source would have if it were opaque and a thermal source. At low frequencies, where the Rayleigh–Jeans approximation applies, the brightness temperature is directly proportional to intensity. Radio Astronomers often work in the units of Brightness Temperature. At low frequencies, where the Rayleigh–Jeans approximation applies, the brightness temperature is directly proportional to intensity. It is given by

$$T_B = \frac{\lambda^2}{2k} I_\nu$$

At higher frequencies, where the Rayleigh Jeans Approximation is not applicable, we need to use the full Planks's Function. In this case, the Brightness Temperature is defined as :

$$B_\nu(T_B) = \frac{2h\nu^3}{c^2} \frac{1}{e^{\frac{h\nu}{kT_B}} - 1}$$

2.3 Why Radio Telescopes are Based on ground ?

In the module of radiation physics, we learned about the adsorption bands.The gases that comprise our atmosphere absorb radiation in certain wavelengths while allowing radiation with differing wavelengths to pass through.The areas of the EM spectrum that are absorbed by atmospheric gases such as water vapor, carbon dioxide, and ozone are known as absorption bands.The ability of the atmosphere to allow radiation to pass through it is referred to as its transmissivity, and varies with the wavelength/type of the radiation.In the figure, absorption bands are represented by a low transmission value. From the figure (2.1), we can see the atmospheric window in radio region of the EM Spectrum.
The radio band contains a large range of frequencies that can travel through the Earth's atmosphere unimpeded and so provides an excellent realm for the detection and study of EM radiation from space. The radio window, as it can be called, ranges in frequency from 10 MHz (1×10^7 Hz) up to 300 GHz (3×10^{11} Hz), or in wavelengths from 30 m down to 1 mm. The energies of

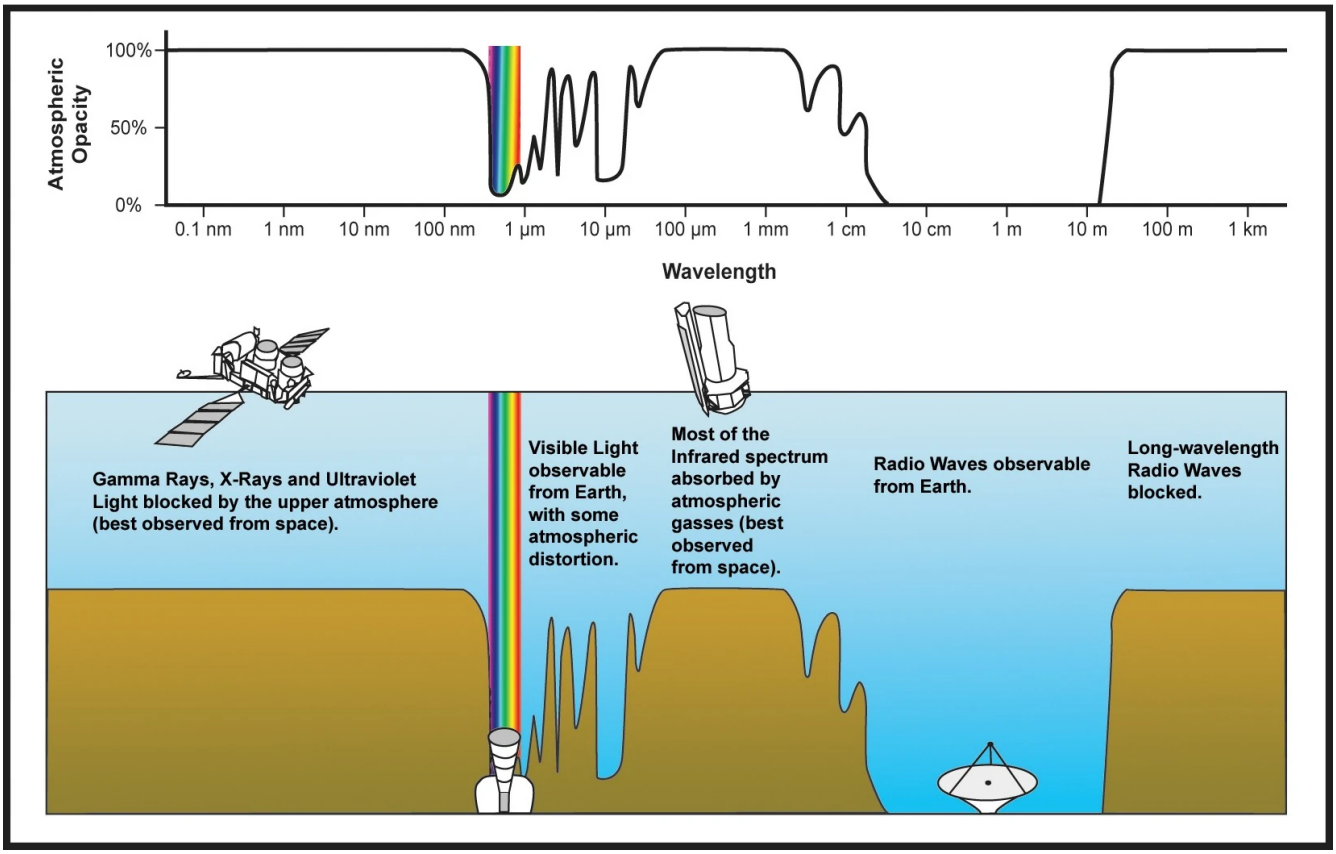

Figure 2.1

radio photons range from about 10–19 to 10–15 ergs—that is, very tiny!!! The boundaries of the radio window are due to atmospheric and ionospheric processes.At low frequencies (below about 10 MHz), free electrons present in the ionosphere easily absorb and/or reflect radiation. Frequencies below this can be generated and transmitted on the Earth's surface, but they cannot escape through the ionosphere. Likewise, waves with frequencies less than 10 MHz arriving from space cannot penetrate the ionosphere to reach ground-based radio telescopes. Frequencies below about 10 MHz must be observed from space-based radio telescopes.

2.4 Why Observe the Universe in Radio Waves ?

To build a more complete picture of the astronomical source under observation, astronomers need to observe it across different frequencies of the EM Spectrum, as they reveal different properties of the Source. Say we are observing a galaxy, different frequencies help us learn about different parts and aspects of the galaxy. At longer wavelengths like Radio Waves, we can see the distribution of interstellar gas (mainly Hydrogen). Whereas, observation in Ultraviolet Spectrum reveals the distribution of high temperature stars in the galaxy, as their radiation spectrum peaks in the Ultraviolet Region.
Figure 2.2 shows the image of Andromeda Galaxy in different parts of the EM Spectrum.

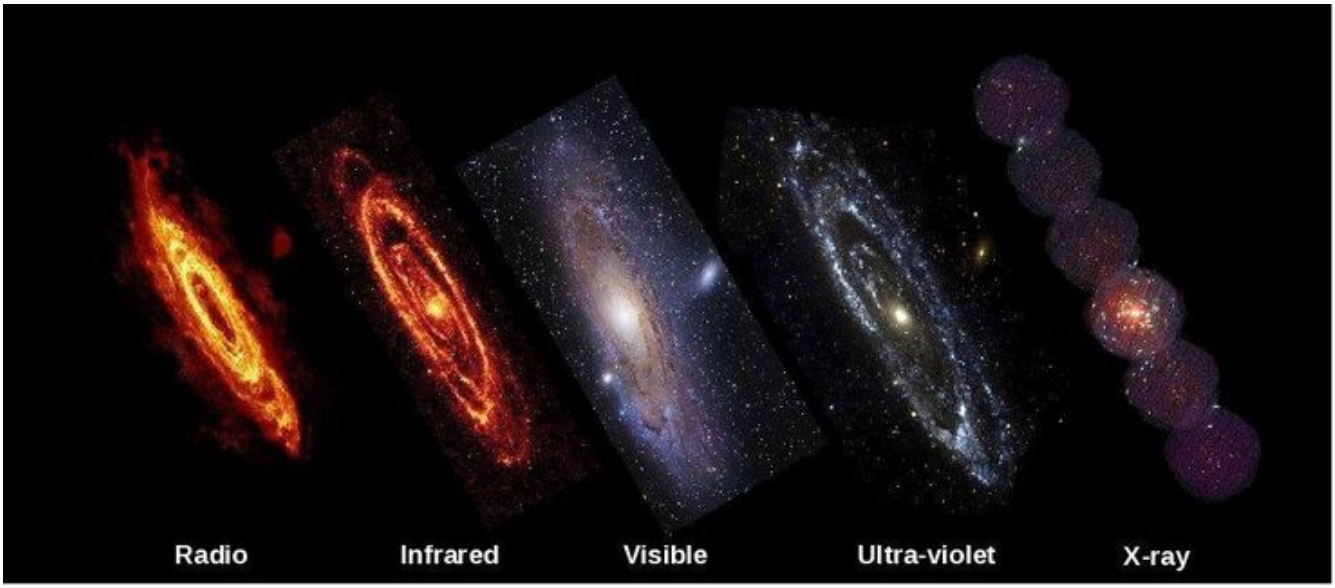

Figure 2.2

2.5 Radio Maps

Showing the structure of a source at radio wavelengths (or at other wavelengths), requires the presenter to make a choice about how best to display the two-dimensional data. The simplest way is with a contour map. The contours are lines of constant intensity. a large number of closely spaced contours in an astronomical map indicate a region where the intensity is changing rapidly with the position. A slightly more intuitive radio map is a gray scale map, in which no color is indicated, and the brightness variations in the source are directly indicated by the shades of gray, where black is the most intense and white is the least. Other way of representing the data is through False Color Maps, in which the color does not indicate different wavelengths but different levels of brightness. These images are usually accompanied with a color-wedge that indicates the relation between color and brightness. These maps look nice and also can significantly facilitate the analysis.

Radio Telescopes

Observing with a radio telescope can be very different from using a visible-wavelength telescope. The Sun does not light up the whole sky at radio wavelengths, as it does at visible wavelengths. The blue daytime sky you see is sunlight that is scattered by the atmosphere, which scatters blue light to a greater extent than the longer visible wavelengths. At radio wavelengths, there is no scattering by the atmosphere at all. Therefore, the daytime sky is dark at radio wavelengths, and so radio observations can be made during day or night. At long radio wavelengths, observations can occur even with a cloud-covered sky since clouds are transparent at these frequencies. At shorter radio wavelengths, though, the water in clouds is a significant source of light loss, and so shorter-wavelength observations require clear weather. Radio telescopes operating at these short-radio wavelengths are often placed in high and dry sites to minimize this loss.

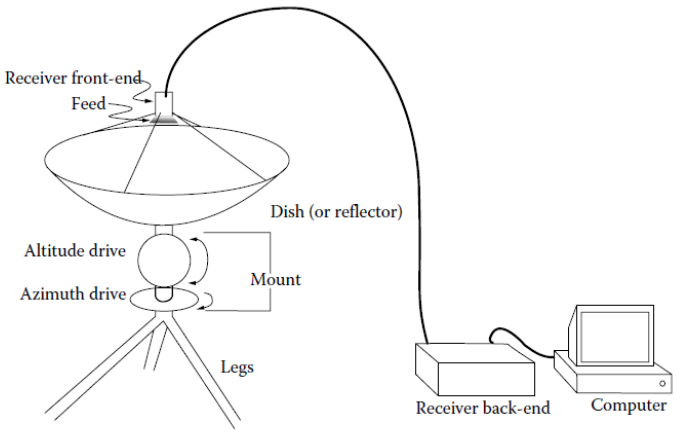

Figure 3.1: A Traditional Primary Reflector Radio Telescope

The component of a radio telescope responsible for collecting the radio signals is often referred to as an antenna or a reflector and these terms are often used interchangeably. There is a difference between the precise meanings of these two terms, however. An antenna is a device that couples electromagnetic (EM) waves in free space to confined waves in a transmission line, while reflectors, which are usually parabolic in shape, collect and concentrate the radiation. Most large radio telescopes employ a reflector as the first element, but they still need an antenna to couple the EM waves into a transmission line, which then carries these waves to the receiver. At long radio

wavelengths, simple *dipole antennas* can be used as the first element. The famous Muchison Widefield Array (MWA) is one such example of a radio telescope, where first element is a dipole antenna. Two other words that are commonly used, and which help to avoid the misuse of the

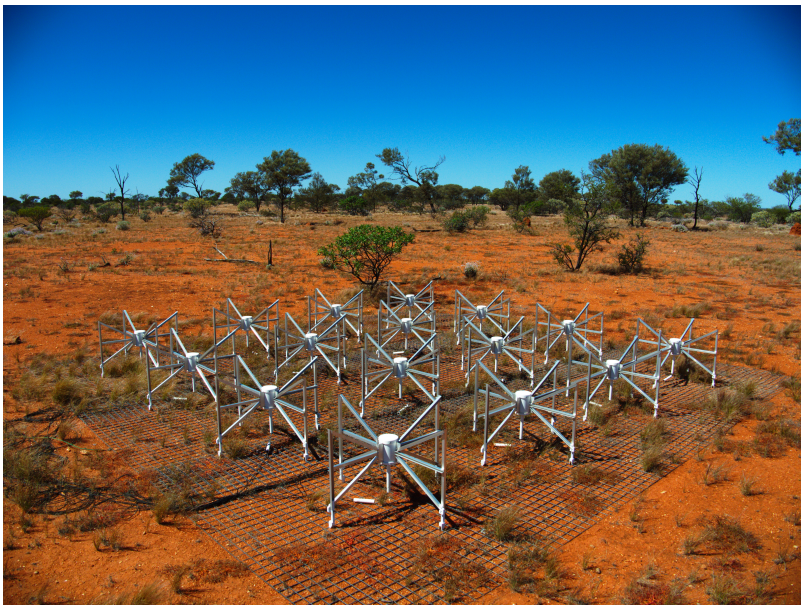

Figure 3.2: Muchison Widefield Array

word antenna, are the dish, which is often used to refer to the reflector, and the feed, which is the device that couples the radiation concentrated by the reflector into a transmission line.

3.1 Primary Reflectors

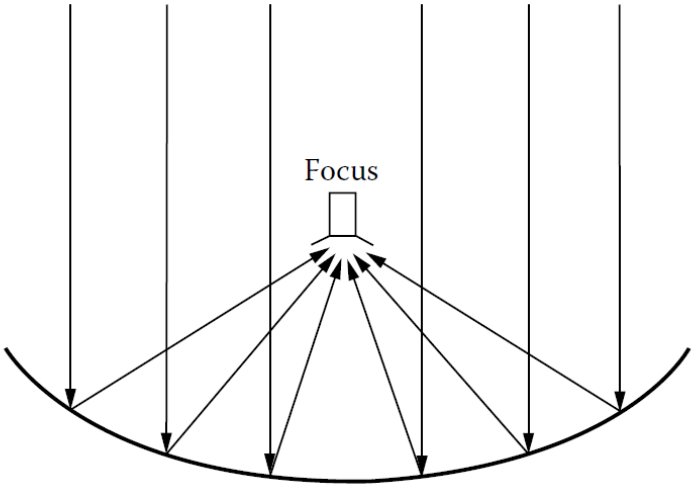

Figure 3.3: Primary Parabolic Reflector

The dishes of most radio telescopes are parabolic reflectors, similar to the primary components in telescopes used in the infrared, visible, and ultraviolet regimes. The parabolic shape causes

all waves approaching the dish from the direction perpendicular to the entrance plane to come to a single point, known as the focus of the telescope. The EM waves emitted by an astronomical object, as they approach our telescope many light years away, are well approximated as plane waves and so enter the telescope in parallel paths.Figure 3.3 depicts the reflection of radio waves off a parabolic reflector and those arriving at the focus point
If the direction of the astronomical source is off the central axis of the reflector, the waves will still converge approximately to a point, but offset from that of an on-axis astronomical source. Therefore, in fact, the parabolic reflector has a focal plane and not just a single focus.
Figure 3.3 shows just one *feed* located at the focus of the telescope.however, multiple feeds are often used to collect the power from different directions simultaneously. The prime-focus configuration can be inconvenient, because the feed and receiver are in an awkward position, located high above the primary reflector and hence not easily accessible when the telescope is aimed at the sky. For this reason, most radio telescopes (and visible-light telescopes as well) are of *Cassegrain* design. In a *Cassegrain* telescope, a second reflector (or mirror) is placed before the focal plane of the primary reflector to redirect the waves to another focal point at or behind the vertex of the primary reflector. This arrangement is shown in Figure 3.4.

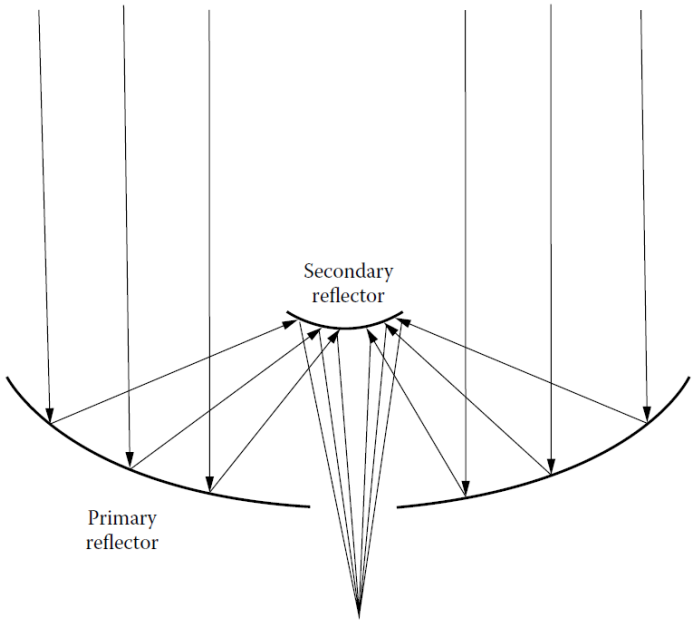

Figure 3.4: Optical Layout of Cassegrian Telescope

The primary reflector serves two important functions. First, it collects and focuses the radiation from astronomical sources, making faint sources more detectable. The amount of radiation collected depends on the telescope's effective area (A_{eff}), which is closely related to the physical area of the primary reflector. As given by Equation 2.2, the power, P, of radiation collected from an astronomical source of flux density F_ν is given by

$$P = F_\nu A_{eff} \Delta\nu$$

Where:
bandwidth, $\Delta\nu$ is the range of frequencies detected.

The bandwidth is determined by the receiver. The larger the physical area of the reflector, the more power is collected from an astronomical source and more readily faint sources can be detected. A number of factors affect the amount of radiation that enters the receiver and so the effective area of a radio telescope is always smaller than its geometrical area.
The second function of the primary reflector is to provide directivity, which is a telescope's ability to differentiate the emission from objects at different angular positions on the sky. When using a single radio telescope to make a map, the directivity determines the resolution in the map. The directivity of a telescope depends, largely, on the diameter of the primary reflector and is governed by the principle of diffraction. Diffraction, in fact, limits the directivity of all telescopes. The directivity of a radio telescope is commonly described as the telescope's beam pattern, which is the topic of the next section.

3.2 Beam Pattern

The beam pattern is a measure of the sensitivity of the telescope to incoming radio signals as a function of angle on the sky. This is similar to what optical astronomers often call the point-spread function. The term beam pattern derives from the idea of a beam of radio waves leaving a transmitting antenna. Because the sensitivity pattern is the same, whether the antenna receives or transmits—a principle known as the reciprocity theorem—we are free to describe the pattern either way. Ideally, we would like each feed in our telescope to collect radio signals from only one direction in the sky, so that when we point the telescope in a specific direction, the power detected through each feed corresponds to the radiation coming from only that spot in the sky. Unfortunately, this is not possible due to the diffraction of light. Consider a prime focus telescope

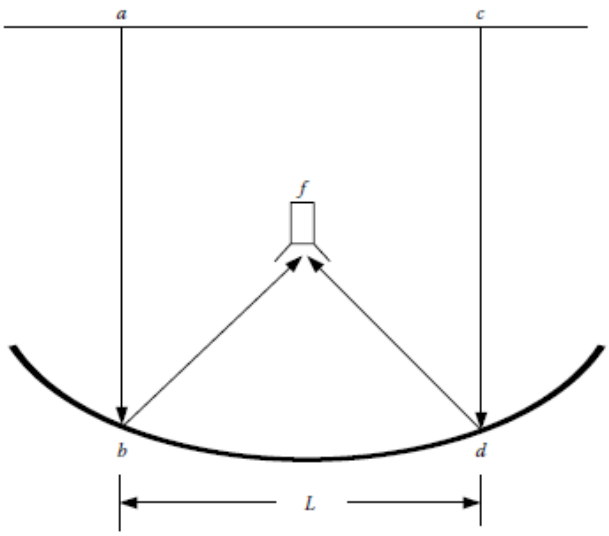

Figure 3.5: Path of two light rays, which reflect off two points on the primary reflector (b and d) and meet at the prime focus.

as depicted in Figure 3.5. Light from a distant astronomical source appears as a continuous chain of plane waves and the parabolic reflector brings these light rays to a single focus. Figure 3.6 shows the light rays from an astronomical source located along the optical axis of the telescope, that is, in

the direction where the telescope is pointed. To simplify the calculations, we consider first only the contributions from two points on the reflector. The plane waves reflecting off the primary reflector at points b and d, which are separated by distance L, arrive at a common focus at point f. Note that for an on-axis source, the wave fronts are perpendicular to the optical axis and therefore the path length *abf* is equal to the path length *cdf*. Therefore, the phases of the waves from these two points are identical (see Figure 3.1, which shows the behavior of the wave fronts) so the waves add constructively at the focus. What happens to slightly off-axis plane waves, such as those coming

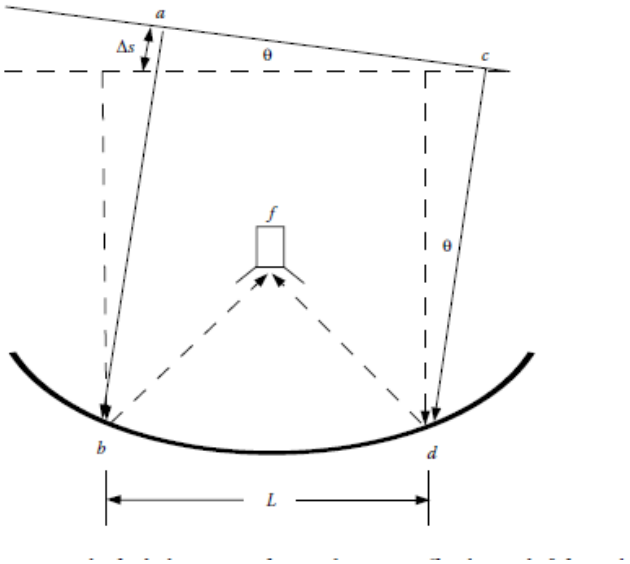

Figure 3.6: Path of two light rays, which reflect off two points on the primary reflector (b and d) and meet at the prime focus.

from a source that is not along the optical axis? The ray tracing for off-axis waves is shown in Figure 3.6. The plane waves are now not perpendicular to the optical axis, but are tilted by an angle θ. In this case, the path length abf is slightly longer than the path length cdf. Since lines ac and ab are perpendicular, $sin\theta = \Delta s/L$, and so the path length difference, Δs, is given by the distance from point a to the horizontal dashed line ,

$$\Delta s = Lsin\theta$$

For a source located at a small angle, θ, from the telescope axis, we can use the small angle approximation for angles expressed in radians, that is,

$$sin\theta \approx \theta$$

Therefore, the path difference is approximately,

$$\Delta s \approx L\theta$$

Because of this path difference, there is now a phase difference between these two rays of light when they arrive near the focus. Expressing the phase difference, $\Delta\phi$, in radians (remember that there are 2π radians in a complete cycle) gives

$$\Delta\phi = 2\pi\frac{\Delta s}{\lambda} = 2\pi\frac{L\theta}{\lambda}$$

If the path difference, Δs, is $\frac{\lambda}{2}$, then the phase difference will be π radians, and the waves will be exactly out of phase and will cancel at the focus. This destructive interference occurs when the off-axis angular distance is

$$\theta = \frac{\lambda}{2L}$$

We have only considered light from two opposing points on the reflector. When the rays reflect off all other points are also included, one finds that the cancellation is not complete, although the intensity is greatly reduced from when the source is located on-axis.Total destructive interference occurs for the sum of all the rays when the source is located at $\frac{\lambda}{D}$ radians from the central axis, where D is the distance across the aperture. For a uniformly illuminated circular aperture, like that of a typical optical telescope, the total collected power is zero when the source is $1.22(\frac{\lambda}{D})$ radians from the central axis. A sample plot of the sensitivity of a parabolic reflector as a function of angle is shown in Figure 3.7. The telescope's sensitivity pattern, like that shown in Figure 3.7,

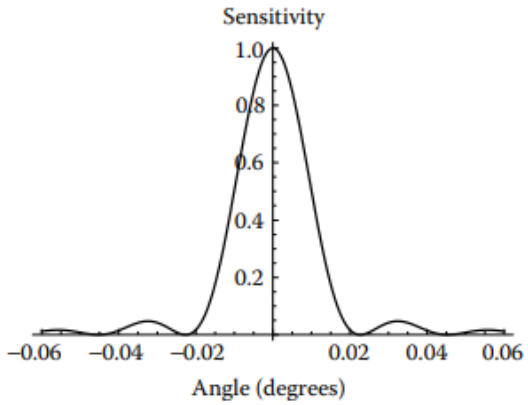

Figure 3.7: Sensitivity Pattern of a Typical Telescope

is called the Airy pattern. The central peak of the sensitivity pattern is called the *main beam.*A telescope, then, can detect power from a source a good ways off-axis, although with much less sensitivity. As the off-axis angle increases further, the response of the telescope goes through a series of peaks and valleys in which there is partial constructive and destructive interference. These off-axis responses are called sidelobes and are undesirable as they can add confusion to observations. The width of the central peak of the Airy pattern is used to define the angular resolution of a single-dish telescope. By convention, the angular width of this peak is taken to be equal to Full Width at Half Maxima(FWHM) of the peak. FWHM is equal to $\frac{1.02\lambda}{D}$, (where D is the distance across the aperature) which is smaller than the radius of the Airy Disc, which is $\frac{1.22\lambda}{D}$. In Radio Astronomy, FWHM of the central Airy Peak is used to define the resolution angle of the telescope. This means, that if two sources lie within this angle, the telescopes sees them as one single source in the sky.Since the FWHM of the main lobe is inversely proportional to the diameter of the reflector, we have that large diameter telescopes not only collect more power from an astronomical source, but also provide better angular resolution. The sensitivity of a Radio Telescope can also be increased by having longer integration times of observation, which can be calculated using Radiometer Equation, which we will come back to later.

3.3 Feeds

At the focus of the telescope, we need antennas to couple EM Waves form space to confined waves in transmission lines for signal to be transmitted to the receiver. These feeds are generally in the shape of horns.They are often flared, , with the radiation entering the larger end and tapering down to the proper size for a type of transission line called the w*waveguide*. The larger end of the flare horn should be of at least the size of one wavlength of the radiation being received. The minimum size of a feed horn opening at long wavelengths, then, can be quite large, thus limiting the number of feeds that can fit in the focal plane of a radio telescope. The radiation reflected off the dish enters the feed horn through a finite-sized opening, approaching from many different angles, and is then combined inside the feed. Diffraction, therefore, again determines the amount of power the feed collects and passes onto the receiver. The beam pattern of the feed determines the *illumination pattern* of the primary reflector.
A quantity that describes how the feed horn's beam is distributed on the primary reflector is called the edge taper, which is defined as the ratio of the sensitivity at the center of the reflector to that at the edge. The shape of the illumination pattern on the primary reflector affects (1) the angular

Figure 3.8: Example of a Circular Feed Horn

resolution of the telescope, (2) the sensitivity level in the sidelobes, and (3) the effective collecting area of the telescope.
. On one hand, with a large edge taper much of the power coming from the outer regions of the reflector is not detected, and so the effective collecting area of the telescope is reduced. The ratio of the effective collecting area considering this effect to the physical area is called the illumination efficiency. On the other hand, with a small edge taper, since the illumination is still fairly large at the edge of the reflector, some of the feed's beam pattern misses the reflector, and so the signal entering the feed is diluted by its sensitivity to area beyond the physical reflector. The illumination of the feed beyond the reflector is called spillover. Thus, a large edge taper optimizes the spillover efficiency, while a small edge taper optimizes the illumination efficiency. The maximum collecting area results from a compromise between spillover and illumination efficiency. The edge taper that maximizes the collecting area of the telescope is one in which the power per unit area transmitted to the center of the reflector is 10 times larger than that at the edge; this is called a 10-dB edge taper.
With regard to angular resolution and sidelobe levels, A large edge taper minimizes the sidelobe level, but produces poorer angular resolution, whereas a small edge taper increases resolution of the telescope but also increases the sidelobe levels. The edge taper that maximizes the effective

collecting area, the 10-dB taper, fortunately, is also a good compromise between good resolution and low sidelobe level. The FWHM of the central Airy Peak with 10-dB taper is given by:

$$\theta_{FWHM} = \frac{1.15\lambda}{D}$$

For this optimum edge taper, the first sidelobe level is approximately 0.4 percent of the peak, and the maximum collecting area of the telescope is about 82 percent of the reflector's physical area.

3.4 Surface Errors

The primary reflector of a radio telescope is never a perfect parabola. There are always manufacturing imperfections that limit its surface accuracy. We can characterize an imperfect reflector by the root mean square (rms) deviations,δz, of the real surface from that of an ideal parabola measured parallel to the optical axis. Such deviations will cause the path length to the focus to be slightly different for various parts of the reflector. This effect is sketched in Figure 3.9. As we saw in earlier path differences cause phase differences that produce less than full constructive interference; therefore, these deviations reduce the power collected by the telescope. Because the light is reflected off the surface, the total path difference is twice the deviation, $2\delta z$; therefore, these deviations produce rms phase errors of $4\pi\frac{\delta z}{\lambda}$.

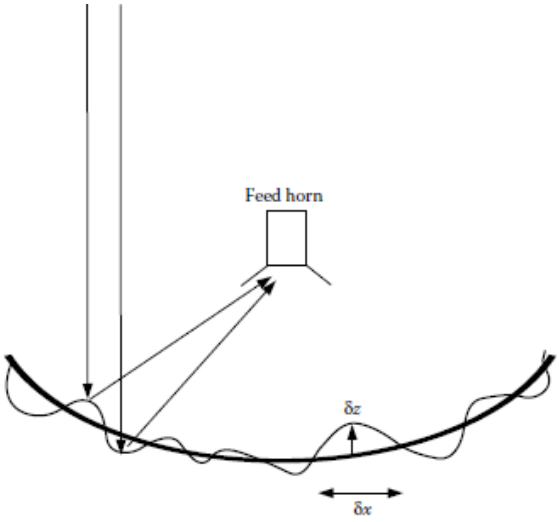

Figure 3.9: Surface irregularities on the reflector cause deviations from a perfect parabola with rms values δz and δx in the directions parallel and perpendicular, respectively, to the optical axis

The presence of surface errors therefore reduces the on-axis sensitivity of the telescope, and this can be viewed as a loss in the collecting area. The effect of surface errors on the collecting area is described by the *Ruze* equation, which is given by

$$A_\delta = A_0 e^{-(4\pi\delta z)^2}$$

3.5 Noise,Noise Temperature and Antenna Temperature

Characterizing noise signals generated in electrical circuits has, of course, always been of great interest in electronics.Nyquist in 1928, for example, found that a resistor in the circuit will add electrical noise with a power per Hz that depends solely on the resistor's temperature. For this reason, the electronic power in a circuit, in general, can be described in terms of an equivalent temperature, T_{equiv}, which is equal to the temperature of a resistor that would produce the same amount of power as the resistor. Following this convention, radio astronomers also describe the power traveling in the transmission lines and receiver in terms of an equivalent temperature given by

$$T_{equiv} = \frac{P}{k\Delta\nu}$$

Where,
k is the Boltzmann Constant and
$\Delta\nu$ is the Bandwidth of the Radiation with Power P. Some of the detected power is due to the astronomical source, which was converted by the antenna to electronic power in the transmission line. We call the equivalent temperature of the power that the antenna delivers to the transmission line, the antenna temperature, T_A. The far majority of the detected power, though, is due to noise from the receiver components. We describe the total noise power by the noise temperature, T_N, and each component in the receiver is characterized by its own noise temperature. Both the source signals and the noise are affected by the amplification and losses that occur along the path through the receiver. The equivalent temperature of the final power output, then, is not simply the sum of the equivalent temperatures of all the sources in the path.
Let us first focus on the signal from the astronomical source and see how its power is affected by the processes in the receiver. At each stage, the source signal is either amplified (when passing through an amplifier) or reduced by a loss (such as in a transmission line). We can use the gain, G for each step; when passing through an amplifier, $G > 1$, and when there is a loss, $G < 1$. For example, if we assign a gain of G_1 to the first element, which is the RF amplifier, then the power in the source signal after this stage is

$$P = G_1 k\Delta\nu T_A$$

Note that the antenna temperature describes the power in the input radiation before any amplification. Even though the amount of power increases when the signal is passed through an amplifier, the radiation is still described by the same equivalent temperature. Therefore, regardless of the amount of amplification in the system, the input radiation power will still be described by the same antenna temperature. An amplifier's noise temperature is defined by the equivalent temperature of the noise power as if it was introduced at the input to the amplifier, and hence it is amplified along with the astronomical signal. Then, the Power Output P would be

$$P = G_1 k\Delta\nu(T_A + T_N)$$

If we have two amplifiers in succession, the first characterized by G_1 and T_{N1}, and the second by G_2 and T_{N2}, then the noise power due to the first is amplified by a factor of G_2 along with the noise produced by the second amplifier. So the total noise power coming out of the second amplifier is

$$P_N = G_1 G_2 k\Delta\nu T_{N1} + G_2 k\Delta\nu T_{N2}$$

The total gain in succession of devices is therefore just a product of individual gains. Now, if for a succession of devices, we define the *total noise temperature* T_N by

$$P_N = Gk\Delta\nu T_N$$

Where, G is the total gain as described above.
Now it remains a trivial calculation to arrive at the formula for *total noise temperature* (just compare the expressions for total noise power) which is given by

$$T_N = T_{N1} + \frac{T_{N2}}{G_1} + \frac{T_{N3}}{G_1 G_2} + ...$$

With total gain and total noise temperature defined, we can define total detected power as :

$$P = Gk\Delta\nu(T_A + T_N)$$

Therefore, even if we observe blank sky, the power out of the receiver is not zero because of the noise power. For these reasons, we cannot readily make total power measurements, but instead, we must make switched power measurements in which we measure the difference in voltage between when the telescope is aimed at the astronomical source (called an on-source observation) and when it is aimed at blank sky (called an off-source observation).It is tempting to believe that the switched observations completely subtract off the noise power, and hence that noise is not really a concern. However, this is not the case. The switched observations remove the offset in the measured power caused by the noise, but the fluctuations in the noise power still affect our measurement and dominate our uncertainty in the antenna temperature. It is these fluctuations that limit the sensitivity of a radio telescope to detect a faint astronomical source. Therefore, we will take a slight disgression into statistics of noise power.

3.5.1 A Brief Statistical Analysis of Noise Power

First, recall that the variance is the mean square deviation from the average. Following common convention, we will use σ to indicate the standard deviation, and thus σ^2 as the variance.Now, when measuring the amount of power in EM radiation, the variance in the measure of that power depends on two effects. Since the amount of power in the radiation is proportional to the number of photons arriving per second, the variance in power must relate to fluctuations in the arrival rate of the photons. The power in the radiation is also proportional to E^2 in the waves, and so the variance also depends on the fluctuations in the waves. The former effect is a consequence of the particle aspect of light while the latter is often called the wave noise and is a purely classical effect. When both effects are included in the statistics, the variance is found to have two terms; the variance due to fluctuations in the photon arrival rate depends on the number of photons per mode (with units of photons per second per Hz) and the wave noise depends on the number squared. More specifically,

$$\sigma^2 \propto n^2 + n$$

Where, n is

$$n = \frac{1}{e^{\frac{h\nu}{kT}} - 1}$$

Therefore, at higher frequencies , the first term of the equation dominates and σ is directyl proportional to the square root of number of photons per mode, whereas, at low frequencies, the second

term of the equation dominates, and σ is proportional to number of photons per mode.
Now, with the necessary background, we can talk about the *Radiometer Equation* mentioned in the section 3.2. We know that with any measurement involving random errors, the uncertainty in the measure decreases by averaging more values, by a factor equal to the square root of the number of measurements. Similarly, by making the measurement for more seconds or by increasing the bandwidth, we make many independent measurements of the power. In general, the number of independent measurements (or modes) made over a time period of Δt and bandwidth $\Delta\nu$ is given by $\Delta t\Delta\nu$. Therefore, in an observation with a bandwidth $\Delta\nu$ and integration time of Δt, the uncertainty in the power measured, σ_P, is given by

$$\sigma_P = \frac{P_N}{\sqrt{\Delta t \Delta \nu}}$$

This is the Radiometer Equation and is essential for planning of any radio observation.

Aperture Synthesis (Inteferometry) - A Quest for Resolution

We discuss the extremely important observing method known as *aperture synthesis*. This technique uses a large number of telescopes arranged in an array in order to produce high-resolution images. In this chapter, we consider a simplified situation to illustrate the basic idea of how the technique works and highlight its fundamental principles.The importance of aperture synthesis cannot be overstated. It has had a profound impact on radio astronomy and the studies of the universe. In recognition of its importance, half of the 1974 Nobel Prize in Physics was awarded to Martin Ryle for his development of the method; the other half was awarded to Anthony Hewish for the discovery of pulsars. Some famous Radio Telescopes based on the principle are The Giant Meterwave Radio Telescope (GMRT) located in Pune, The Jansky Very Large Array in San Agustin, New Mexico and the Atacama Large Millimeter/Submillimeter Array (ALMA) located in the Atacama Desert in the Andes of Northern Chile.

Figure 4.1: Jansky Very Large Array in San Agustin, New Mexico

Figure 4.2: Giant Meterwave Radio Telescope in Pune, India

Figure 4.3: Atacama Large Millimeter/Submillimeter Array (ALMA) located in the Atacama Desert in the Andes of Northern Chile

4.1 Why Aperture Synthesis ?

The main advantage of aperture synthesis is angular resolution. The long wavelengths of Radio Astronomy limit the single-dish observations to very poor resolution. Ground-based observations at visible wavelength can obtain a resolution of 1 arcsec, or 2×10^{-5} radians. For a Radio Telescope

to match this resolution, its diameter has to be approximately (using the equation for θ_{FWHM}) :

$$D \approx \frac{10cm}{2 \times 10^{-5}} \approx 5km$$

Building a dish with that huge a diameter will involve a lot of engineering complications and is practically not feasible.radio astronomers can achieve this resolution by combining a number of ordinary-sized radio telescopes. With the radio telescopes laid out in an array and treating each pair of telescopes as an interferometer, we can effectively synthesize a new telescope with a very large diameter. This is done by observing the same source with all telescopes in the array, combining the outputs from each pair of telescopes, and mathematically processing the data in a way that produces the equivalent resolution of a single large telescope. The result of this process is an effective resolution that is approximately equal to that of a telescope whose diameter equals the largest distance between antennas in the array.Keep in mind that aperture synthesis produces only the resolution of a large telescope, not the sensitivity. The sensitivity depends on the total collecting area, which, for an array of antennas, is the sum of the effective areas of all the individual antennas.

4.2 Two Element Interferometer

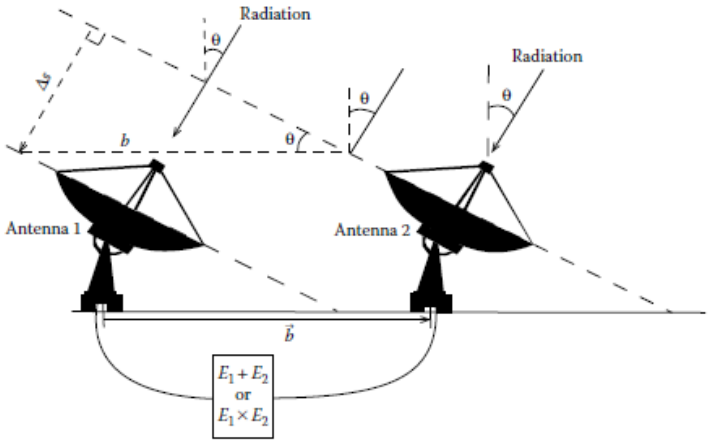

Figure 4.4

The basic unit of an aperture synthesis telescope is the two-element interferometer, composed of two antennas separated by a well-known distance with a well-known orientation. The vector describing the separation of the antennas is known as the baseline, which we will symbolize as $\vec{b}$. In an observation, both antennas are pointed at the astronomical source, which is located in some direction on the sky that can be defined relative to the zenith of the midpoint of the baseline. To simplify the discussion in this chapter, we will consider a special case in which the source, the antennas, and the zenith of the baseline midpoint are all contained in the same plane. This is the case, for example, if the interferometer is on the Earth's equator, has an east–west baseline, and the source is located on the celestial equator. In this case, when the source transits, it passes through the zenith of the interferometer; the source direction, then, can be described by a single

angle, θ, relative to the zenith. Additionally, this constrains the baseline to only one possible orientation, and so the distance, $\vec{b}$, between the antennas, will suffice to describe the baseline.

A depiction of an interferometric observation in this two-dimensional situation is shown in Figure 4.4. The radio signal from an astronomical source in direction q relative to the zenith approaches both antennas along parallel paths, since the source is, effectively, infinitely far away. The antennas respond to the oscillating electric fields, $E_1(t)$ and $E_2(t)$, of the electromagnetic waves, which are filtered to pass a small bandwidth centered at some specific frequency, ν, and then sent along identical cables where they meet and are combined.
Using the right triangle shown in Figure 4.4, we can express the delay in terms of the direction toward the source. The extra distance Δs is one side of the right triangle in which b is the hypotenuse. So by simple trigonometry, $\Delta s = bsin\theta$, or

$$\tau = \frac{bsin\theta}{c}$$

This time delay in the arrival of the wave front means there will be a phase difference, $\Delta\Phi$, between the two signals, given by

$$\Delta\Phi = \frac{2\pi\Delta s}{\lambda}$$

If Δs equals one wavelength, then the wave front entering antenna 2 will be 2π radians ahead of the same wave front entering antenna 1. We can also express the phase difference in terms of the time delay by

$$\Delta\Phi = 2\pi\nu\tau$$

If we choose the time when the wave enters antenna 1 as defining zero phase, then we must add the phase shift to the wave entering antenna 2 (to make it further along in its cycle before combination). Therefore, we have that the electric fields arriving at the combination point are given by

$$E_1 = E_0 cos(2\pi\nu t)$$

$$E_2 = E_0 cos(2\pi\nu(t+\tau))$$

We note that due to the Earth's rotation, the angle θ will slowly change with time, and so will the phase difference or time delay between the signals from the two antennas. To Calculate the net response we add or multiply these two signals and then take average. To Illustrate, Here we show the multiplicative response, the additive response is left as an exercise to the reader. We disuss multiplicative interferometer, because almost all modern interferometers are multiplicative as they much less affected by noise as compared to additive interferometers.

4.2.1 Response of Multiplicative Interferometer

Multiplying the Electric Fields entering the two antennas , we get

$$E_1.E_2 = E_0^2 cos(2\pi\nu t)cos[2\pi\nu(t+\tau)]$$

Using Basic Trigonometry, we can write this as

$$E_1.E_2 = \frac{E_0^2}{2}cos(4\pi\nu t + 2\pi\nu\tau) + \frac{E_0^2}{2}cos(2\pi\nu\tau)$$

The product of the electric fields is averaged over a period of time, called the integration time (the time of observation).The first term averages to zero, and so only the second term remains.
Its very important to note here that the added signals are averaged over time t, while τ, the delay for the wave front to reach antenna 1, is relatively constant over the integration time (although it changes slowly as the Earth rotates). The term $cos(2\pi\nu\tau)$, therefore, does not go to zero when time averaged.
Therefore, the detected power of multiplicative interferometer is :

$$\langle E_1.E_2 \rangle = \frac{E_0^2}{2} cos(2\pi\nu\tau)$$

The delay is related to the extra path length by $\tau = \frac{\Delta s}{c}$, where $\Delta s = bsin\theta$, allowing us to write

$$\langle E_1.E_2 \rangle = \frac{E_0^2}{2} cos(2\pi \frac{b}{\lambda} sin\theta)$$

4.2.2 Similarity with the Young's Double Slit Experiment

Consider the Young's Double Slit Experiment where light is emitted from two slits and forms a fringe pattern on the screen. Note that the fringe width is proportional to $\frac{\lambda}{D}$ where D is the distance between the **slits**.

Now a Radio Telescope is basically an antenna that is converting electromagnetic signals in the space to electrical signals in wires. It follows from symmetry(or more formally, the Reciprocity Theorem) that these receiving characterstics are similar in nature to the radiation characterstics. Thus a two element radio interferometer is in essence just like the Young's Double Slit experiment, the only difference being that the 'slits' are now receiving light rather than emitting it.

The figure below shows the fringe pattern of two such 2-element interferometers. Superimposed on them are the telescope represented by blue-dots and the distance between them(also called a 'baseline')

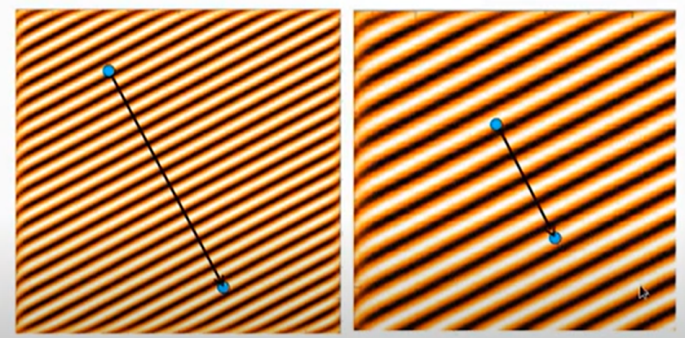

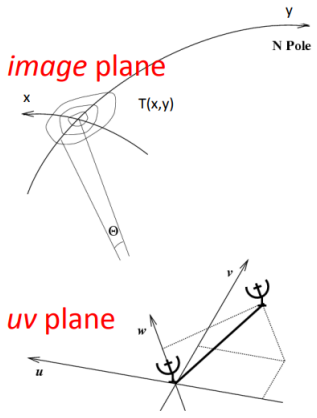

(a) Fringe-pattern of a 2 element interferometer in uv plane

As one observed directly overhead in the middle of the two telescopes, there is a constructive interference. As we move away from the midpoint it starts to destruct until it reaches a minima and then constructs again.

Also notice how as the distance D between the telescopes decreases, the fringe width increases. This fringe pattern can be characterised by the formula

$$cos(ul + vm)$$

where u,v denote the coordinates in the radio telescope frame and l, m in the image frame. u is generally taken to be the East-West direction(the horizontal axis in above fringe pattern diagram) and v to be along North-South Direction(the vertical axis in above diagram)

4.3 Visibility and Fourier Transformation

We define a new term, Visibility V(u, v) which is a complex term and is related to the fringe amplitude and average intensity at a given point u, v on the uv plane.

$$V(uv) = \sum_{ij} V_{ij}(u, v, t, \delta t, \nu, \delta\nu) =< V_i(.., t, ..)V_j^*(..., t + \tau, ...) >$$

Note that the expression for V_{ij} is exactly the same as the result which we calculated in Section 4.2.1, just represented as a complex number to represent both Amplitude and Phase. V(u, v) is just $V_{ij}(u, v)$ summed over all pairs of telescopes.

The Visibility V(u,v) is directly related to the brightness of the source. In particular for small fields of view, it turns out that that the visibility $V(u, v)$ is the 2D Fourier Transformation of the brightness of the sky $T(x, y)$. Thus if we are able to find $V(u, v)$, we can just make an Inverse Fourier Transformation and obtain $T(x, y)$, which is the brightness of the source in the image plane, or in simple words the image of the source!

$$T(x, y) \longleftrightarrow V(u, v)$$

$$V(u, v) = \int\int T(x, y)e^{2\pi i(ux+vy)}dxdy$$

$$T(x, y) = \int\int V(u, v)e^{-2\pi i(ux+vy)}dudv$$

On the next page are some 2D fourier transformation pairs aimed to help in understanding of the relation between $V(u, v)$ and $T(x, y)$. In particular notice the effect of fourier transformation mentioned in the caption.

Thus now our aim is to sample $V(u, v)$ at enough number of (u, v) points using distributed small-aperture telescopes to synthesize a large aperture telescope of size (u_{max}, v_{max}) . How do we do this?

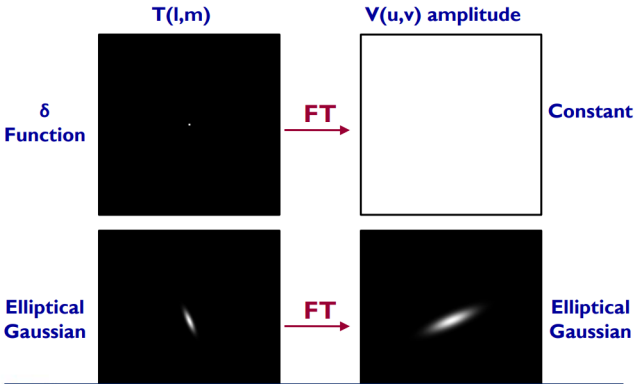

Figure 4.6: Narrow features become wide features and vice-versa

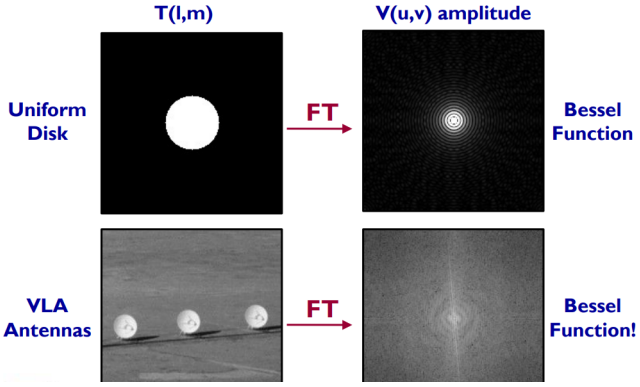

Figure 4.7: Sharp edge in image leads to high spatial frequencies. Even if one ignores the higher frequencies and just takes an Inverse Fourier of the central part of V(u, v), the resulting image is fairly close to the original.

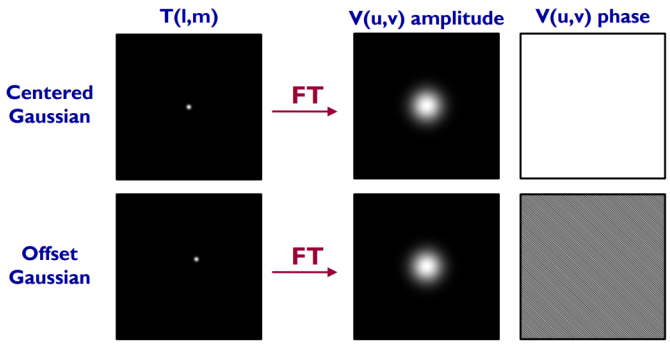

Figure 4.8: Amplitude tells you 'how much' of a spatial frequency, Phase tells you 'where' the spatial frequency is

4.4 N element interferometer

For an interferometer with N telescopes, there are a total of $\frac{N(N-1)}{2}$ baselines possible. For example, for the following array of 4 telescopes, the 6 baselines are shown in red and the vector in the opposite direction in blue.

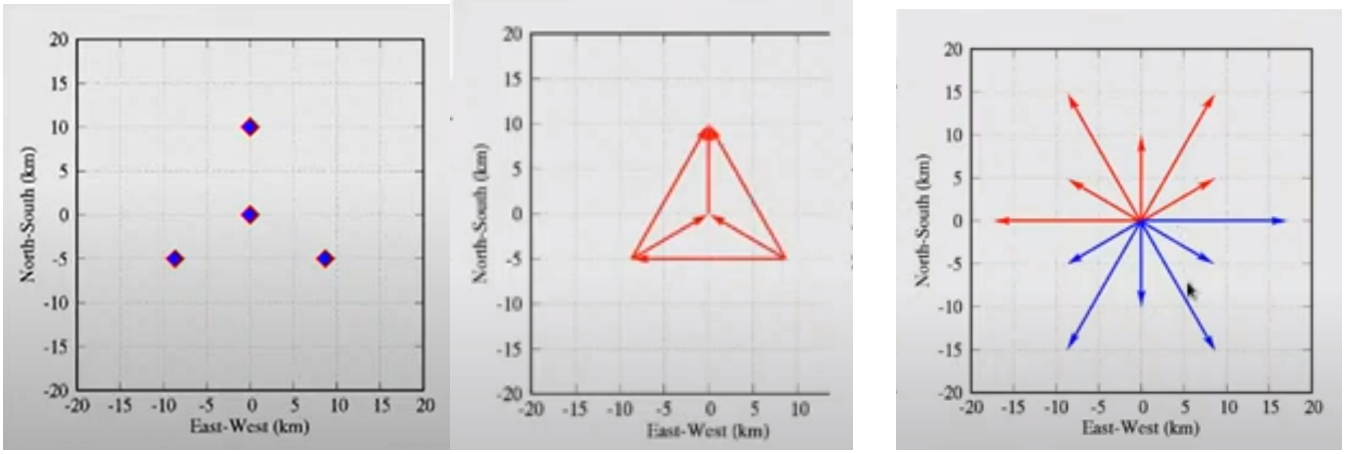

Each of these baselines have a separate fringe pattern characterised as $cos(u_i x + v_i y)$, where u_i, v_i are the projection of the baseline on East-West and North-South direction respectively.
The final response of the interferometer will be the superposition of fringes from all baselines.

You've already seen the interference pattern due to 2 Element Interferometer. As we increase the number of telescopes, more and more fringes superimpose in different direction and we get a different interference pattern. Further, as the earth rotates, the telescopes occupy a new location u, v and increase the u-v coverage. After taking in samples from enough telescopes and allowing the earth to rotate, we obtain an interference pattern with only the center as peak. This is because at the center, the rays always constructively interfere while at other points they average out to zero.
As we cannot measure the visibilities at all points in the u-v plane, we define the set of points (u, v) where we have sampled the image as the sampling function $S(u, v)$.

$$S(u, v) = \sum_k (u_k, v_k)$$

The Point Source Response of an Interferometer is the Fourier Transform of S(u, v). It is also known as the Point Spread Function(PSF) or Dirty Beam.

$$P(x, y) \longleftrightarrow S(u, v)$$

Shown below are the S(u, v) and Point spread configuration for some arrays of telescopes. As the number of sample decreases, the Point Spread Function aptly spreads and leads to a more 'dirty' image.

Thus to have a "good" image you need to have a "good" sampling of the uv plane.

Synthesized Beam (i.e.,PSF) for 2 Antennas

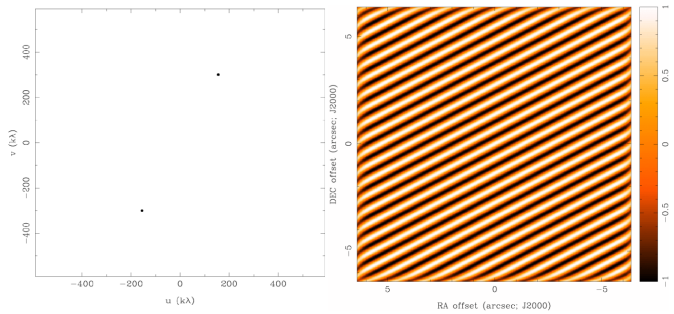

4 Antennas

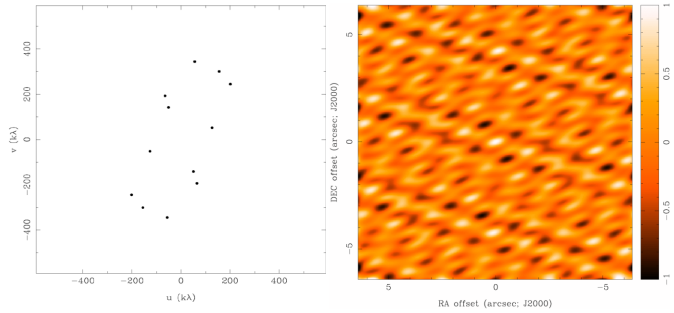

8 Antennas

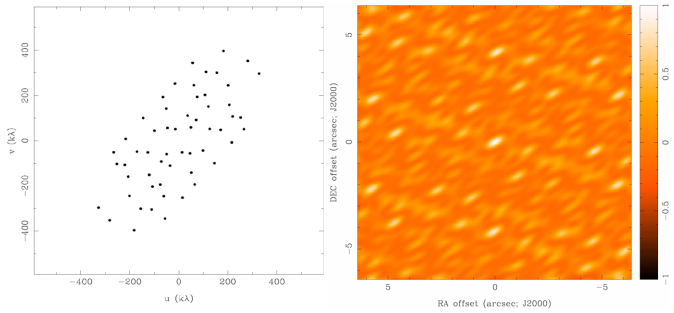

8 Antennas x 240 Samples

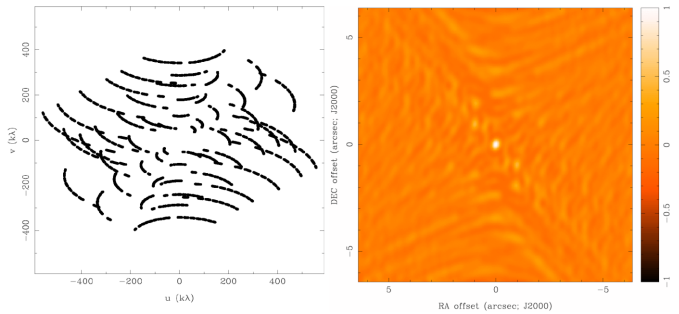

4.5 Synthesis Imaging

Again, as we could not measure the visibility at all points (u, v), we can't calculate T(x, y) exactly, as it requires the values of V(u,v) at all u,v.

Instead what we calculate is

$$T'(x,y) = \int\int S(u,v)V(u,v)e^{2\pi i(ux+vy)}dudv$$

where $S(u,v)$ is the sampling function having the value 1 when we have a sample at (u,v) and 0 otherwise.

This is called the 'Dirty Image'. It can be clearly seen from the Convolution Theorem that the dirty image $T'(x,y)$ is just the convolution of the Point Spread Function and the true sky brightness $T(x,y)$

$$T'(x,y) = P(x,y) * T(x,y)$$

To get the true sky brightness $T(x,y)$, one needs to 'deconvolve' the PSF from the 'dirty image' .

The deconvolution process consists of giving reasonable values to the visibility in the unmeasured (u,v) areas in order to get a nice gaussian beam without sidelobes. The most successful deconvolution procedure is the algorithm CLEAN (Hogbom1974). You can learn more about that here https://adsabs.harvard.edu/full/1999ASPC..180..151C

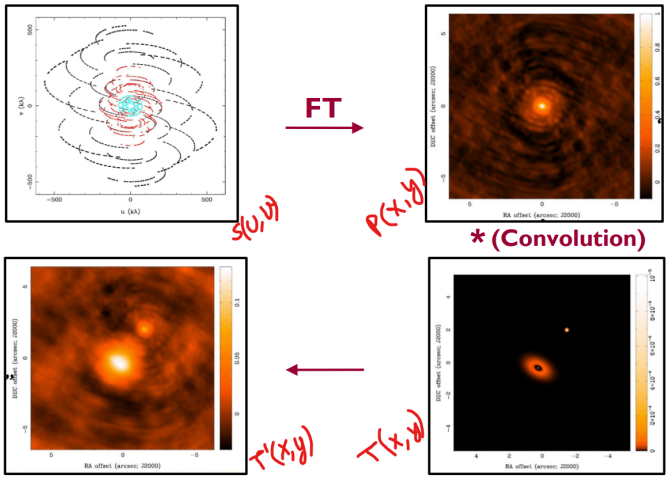

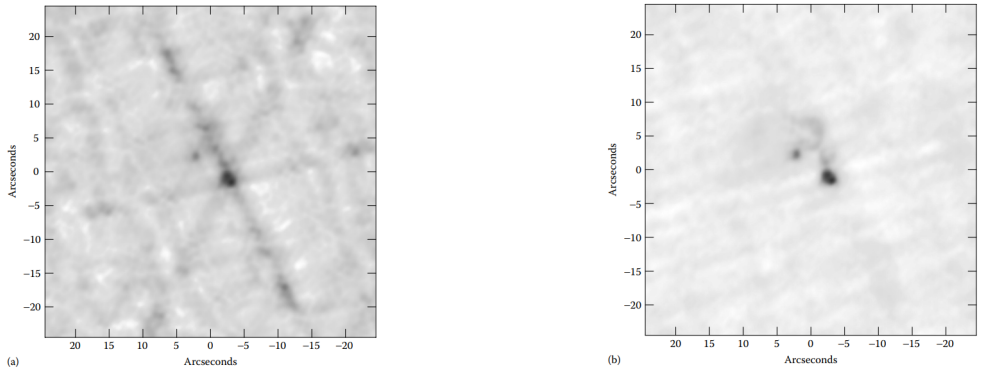

Figure 4.10: Left: A dirty image from an observation with the Janksy VLA. Right: The CLEAN image of the same observation, after the dirty beam has been deconvolved.

Further Reading

1. Radio Astronomy, J. D. Kraus, 1986, Cygnus-Quasar Books, Powell, Ohio
2. Tools of Radio Astronomy, 2nd edition, 1996, K. Rohlfs and T. L. Wilson, Springer-Verlag, Berlin
3. Interferometry and Synthesis in Radio Astronomy – A. R. Thompson, J. M. Moran and G. W. Swenson, 3rd Edition, 2017, Wiley Interscience, New York
(https://link.springer.com/book/10.1007/978-3-319-44431-4)
4. Synthesis Imaging in Radio Astronomy II, Ed. G. B. Taylor, C. L. Carilli and R. A. Perley, 1999, Astronomical Society of the Pacific Conference Series, Vol 180, San Francisco
5. Low Frequency Radio Astronomy, 3rd Ed., Eds. Chengalur, Gupta and Dwarkanath